Electrical Power and Energy Systems 58 (2014) 1–8

Contents lists available at ScienceDirect

Electrical Power and Energy Systems

journal homepage: www.elsevier.com/locate/ijepes

Power losses evaluation of a bidirectional three-port DC–DC converter for hybrid electric system

Laureano Piris-Botalla *, Germán G. Oggier, Andrés M. Airabella, Guillermo O. García

CONICET, Grupo de Electrónica Aplicada (GEA), Facultad de Ingeniería, Universidad Nacional de Río Cuarto, Ruta Nacional # 36 Km 601, X5804BYA Río Cuarto, Argentina

A R T I C L E   I N F O

Article history:
Received 15 March 2013
Received in revised form 18 December 2013
Accepted 23 December 2013

Keywords:
Three-port DC–DC converter
Hybrid electric systems
Power losses
Soft switching

A B S T R A C T

Power losses of a bidirectional three-port DC–DC converter to be used in hybrid electric systems as a function of the voltage conversion ratios and the output power are evaluated in this work. An analysis and characterization of the current on the switches into the whole converter operating range are presented. This analysis allows finding the semiconductor conduction intervals, necessary to calculate the power losses. Such losses are evaluated considering both switching and conduction semiconductor losses as well as those in the transformer. The variables used in this evaluation are voltage conversion ratios and transformer parameters like leakage inductances and turns ratios. Design considerations for the high frequency transformer that allow minimizing the total power losses are proposed. Simulation results are presented in order to validate the theoretical analysis.

1. Introduction

The use of hybrid electric systems has significantly increased due to their potential applications in hybrid electric vehicles (HEVs), renewable energy systems, microgrids, distributed generation systems, among others [1–5]. In HEV applications batteries and supercapacitors are commonly used as energy storages, due to their high energy density and their capacity to absorb or deliver peak power respectively, for example during a regenerative braking [6–8]. In these applications, the energy sources and storage devices, such as batteries and supercapacitors, may present different voltage levels respect to each other and respect to the load [9]. For this reason, it is necessary to incorporate electronic converters as interfaces between the energy sources and the load, to adapt different voltage levels and to carry out an adequate power flow control [10]. A possible solution is the use of multiport converters centralize the power flow control at only one unit in order to minimize size, cost and complexity of the system [11–13].

Different studies on multiport converters are reported in the available literature. For example, in [14,15] a bidirectional three-port DC–DC converter (TPC) is presented as a solution for hybrid fuel cell system and uninterrupted power supply applications. The power flow control consist in controlling the phase shift between the transformer voltages with fixed 50% duty-cycle.

The TPC topology can operates under soft-switching mode, which allows obtaining high efficiency [16], but this mode only can be reached within a reduced operation range, as a function of the voltage conversion ratio and the output power [11]. This is an important drawback in applications where the voltage sources change their value according to the state of charge (i.e. batteries and supercapacitors) [17].

A bidirectional converter as an interface of batteries and supercapacitors for a HEV application is proposed in [18], where the operation under soft switching mode is achieved by means of an auxiliary circuit which works twice in every switching cycle. The power losses analysis includes those produced by the auxiliary circuit. The total losses are compared with a hard switched counterpart, and it can be concluded that the converter efficiency can be increased up to 8%. In [19], an analysis of efficiency for different load conditions is carried out for the same converter topology than that presented in [18]. Soft switching mode is accomplished using a more efficient auxiliary circuit working only once at each switching instant within each switching cycle and therefore it can be concluded that this change in using the auxiliary circuit increases efficiency.

In previous papers, power losses are evaluated considering the DC voltages of the power supplies constant. For the applications considered in this paper, the voltage conversion ratios and output power could vary significantly for different operating conditions, making the evaluation of power losses a more complex problem to solve. Thus, the different operating conditions modify the conduction intervals of the power switches and the switching instants.

In this paper, an evaluation of power losses of the three-port DC–DC converter is presented. This allows obtaining design considerations for the transformer parameters like leakage inductances and turn ratios. As a result, high efficiency under different operating conditions can be obtained.

* Corresponding author. Tel./fax: +54 358 4676255.
E-mail address: lpiris@ing.unrc.edu.ar (L. Piris-Botalla).

0142-0615/$ - see front matter © 2013 Elsevier Ltd. All rights reserved.
http://dx.doi.org/10.1016/j.ijepes.2013.12.021

This work is organized as follows: Section 2 describes the TPC topology, its principle of operation and a characterization of the current waveforms. In Section 3, expressions for the TPC power losses are obtained. In Section 4, power losses are evaluated as a function of leakage inductance and voltage conversion ratios. Section 5 presents simulation results to validate the losses evaluation. Finally, conclusions are drawn in Section 6.

2. Topology description and principle of operation

The TPC topology is shown in Fig. 1. Sources V_1, V'_2 and V'_3 feed the active bridges B_1, B_2 and B_3 which convert the DC voltage into three alternating voltages, v_{T1}, v'_{T2} and v'_{T3}, respectively, to feed the high-frequency transformer, *Tr*. Each bridge can operates as rectifier or as inverter depending on the direction of the power flow. Each switch S_{xw}, shown in Fig. 1, is implemented by a power transistor, T_{xw}, and an antiparallel diode, D_{xw} [17]. The subscripts x and w represent the number of ports and switches, respectively. In this paper, V_1 represents the voltage of a battery bank, V'_2 the voltage of a supercapacitor, and V'_3 load voltage for a hybrid electric system with the particularity that V'_3 should remain constant while V_1 and V'_2 may increase or decrease depending on the operation point.

In this analysis, all the variables and parameters of ports 2 and 3, shown in Fig. 1, are referred to port 1, as follows: $L_{\ell 2} = L'_{\ell 2}/n_2^2, v_{T2} = v'_{T2}/n_2, V_2 = V'_2/n_2, i_{B2} = i'_{B2}n_2, i_{T2} = i'_{T2}n_2$ and $i_{C2} = i'_{C2}n_2$ for port 2 and $L_{\ell 3} = L'_{\ell 3}/n_3^2, v_{T3} = v'_{T3}/n_3, V_3 = V'_3/n_3, i_{B3} = i'_{B3}n_3$, $i_{T3} = i'_{T3}n_3$ and $i_{C3} = i'_{C3}n_3$ for port 3, where n_2 and n_3 are the transformer turns ratios of ports 2 and 3, respectively.

Fig. 2 shows a simplified TPC Δ-equivalent circuit, deduced in [12], which allows simplifying the power flow analysis. In this figure, the ac voltages, v_{T1}, v_{T2} and v_{T3}, represent the voltages generated by bridges, B_1, B_2 and B_3, respectively, and the inductances L_{12}, L_{13} and L_{23} can be deduced as functions of leakage inductances through a $Y - \Delta$ transformation as in [20]. The transformer magnetizing inductance is considered high enough as not to be included in the model [21].

The TPC voltage conversion ratios are defined as follows: $d_{12}=V'_2/(V_1 n_2), d_{13}=V'_3/(V_1 n_3)$ and the angles δ_{12} and δ_{13} are the phase shifts between v_{T1}-v_{T2} and v_{T1}-v_{T3}, respectively.

In [12] it is demonstrated that the power flow can be controlled by manipulating the phase shifts δ_{12} and δ_{13}.

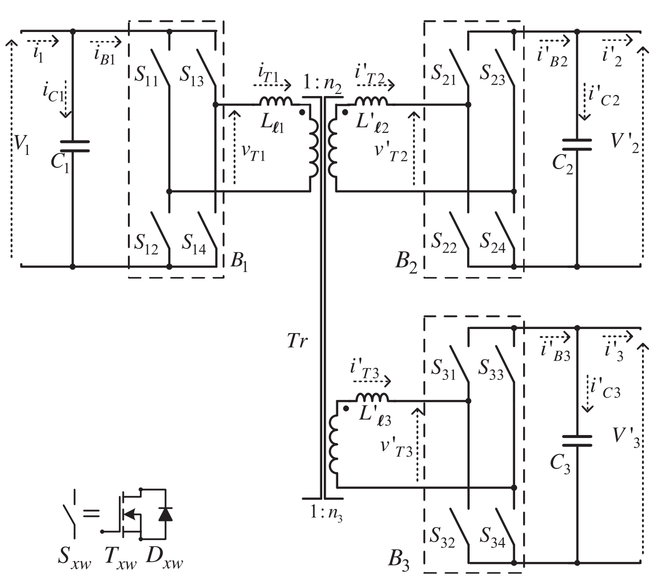

Fig. 1. Three-port bidirectional DC–DC converter topology.

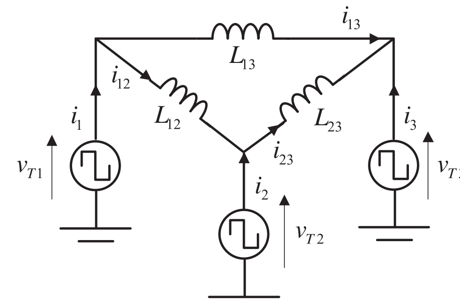

Fig. 2. TPC simplified circuit.

According to the electric equivalent circuit shown in Fig. 2, the dynamics of current along the branches can be expressed as,

$$\frac{di_{xy}(\theta)}{d\theta} = \frac{v_{Tx}(\theta) - v_{Ty}(\theta)}{\omega L_{xy}}, \tag{1}$$

where x and y represent the ports involved in the equation, $\theta = \omega t, \omega = 2\pi f_{sw}$ and f_{sw} is the switching frequency.

Solving (1), the expressions for $i_{12}(\theta), i_{23}(\theta)$ and $i_{13}(\theta)$ (see Fig. 2) can be obtained, which are also used to determine the expressions for currents at each port as follows:

$$i_1(\theta) = i_{12}(\theta) + i_{13}(\theta), \tag{2}$$
$$i_2(\theta) = i_{23}(\theta) - i_{12}(\theta), \tag{3}$$
$$i_3(\theta) = -i_{13}(\theta) - i_{23}(\theta). \tag{4}$$

Based on (2)–(4) the expressions of powers at each port of the TPC can be obtained by solving the following expression [17]

$$P_x = \frac{1}{\pi}\int_0^{\pi} v_{Tx}(\theta) i_x(\theta) d\theta. \tag{5}$$

In order to simplify notation, inductances of the Δ-equivalent circuit are normalized respect to L_{12}, as $L_2 = L_{23}/L_{12}$ and $L_3 = L_{13}/L_{12}$. Thus, the expressions for powers shown in Table 1, can be obtained as a function of V_1.

2.1. Current waveforms characterization

Fig. 3 shows the main waveforms corresponding to the equivalent circuit shown in Fig. 2: v_{T1}, v_{T2} and v_{T3}; the branch currents $i_{12}(\theta), i_{23}(\theta)$ and $i_{13}(\theta)$ and the current at each port $i_{1-a}(\theta), i_{2-a}(\theta)$ and $i_{3-b}(\theta)$ for a particular operating point given by $1 < d_{13} < d_{12}$ and $0 < \delta_{12} < \delta_{13}$. The subscripts a and b represent different cases of operating conditions which will be detailed further on.

From the same figure, it is possible to define the current stages I, II and III when $0 < \theta \leqslant \delta_{12}, \delta_{12} < \theta \leqslant \delta_{13}$ and $\delta_{13} < \theta \leqslant \pi$, respectively. The angle β_{ix-z} corresponds to $i_x(\theta)$ zero crossing of the z current stage. The voltage nominal values at the transformer terminal are represented in dotted lines and solid lines correspond to a particular V_1 and V'_2 DC voltage level when $d_{13} < d_{12} < 1$. This figure also shows the conducting devices at each interval.

Considering a constant DC voltage at the load port V'_3, the voltage conversion ratios, d_{12} and d_{13}, may change as functions of the state of charge of the power sources. In order to obtain a constant output power, variables δ_{12} and δ_{13} have to be adjusted when the voltage conversion ratios change. This results in different current waveforms which modify the limits of the semiconductor conduction intervals.

To determine all possible conduction intervals, it is necessary to calculate the zero crossing angles at the current ports for each active circuits. Fig. 3 and Fig. 4(a) to (d) show all the possible current